PEAK-SPLITTING IN THE RESPONSE OF THE LEAKY INTEGRATE-AND-FIRE NEURON MODEL TO LOW-FREQUENCY PERIODIC INPUTS

Levin Kuhlmann[1,2,*], Anthony Burkitt[2], and Graeme M. Clark[1,2]

[1] Department of Otolaryngology, The University of Melbourne, Royal Victorian Eye and Ear Hospital, 32 Gisborne Street, East Melbourne, VIC 3002, Australia
[2] The Bionic Ear Institute, 384-388 Albert Street, East Melbourne, VIC 3002, Australia
[*] l.kuhlmann@medoto.unimelb.edu.au

Abstract - **The cause of peak-splitting in the output phase distribution of the leaky integrate-and-fire single neuron model in response to low-frequency periodic nerve fibre inputs is analyzed. It is found that peak-splitting largely arises from an increase of the spiking-rate of individual nerve fibre inputs, or from an increase in amplitude of individual input excitatory postsynaptic potentials, or both. These findings add another dimension to the understanding of how peak-splitting arises in the phase histograms of the responses of neurons in the auditory pathway, given that peak-splitting is typically thought to arise as a result of the non-linear dynamics of the basilar membrane and the hair cells. This research has implications for the understanding of the temporal code in the auditory pathway.**

Index Terms - **auditory pathway, leaky integrate-and-fire neuron model, peak-splitting, temporal coding**

I. INTRODUCTION

When stimulating auditory nerve (AN) fibres with a low-frequency ($\leq$ 1 kHz) tonic sound stimulus, in most cases there is only a single peak in a phase histogram constructed on the period of the low-frequency tone [1]. In some cases, however, when the stimulus intensity is increased, two or even three peaks can be seen in the phase histogram [1]. *Peak-splitting* is the term given to this peak multiplication that occurs within a phase histogram when there is an increase in intensity of a low-frequency tonic sound stimulus [1], [2], [3]. The work done on peak-splitting in the auditory pathway has concentrated on inner hair cells (IHCs) of the cochlear [4], [5] and AN fibres [1], [2], [3], [4], [6], [7], [8], [9].

An understanding of the causes of peak-splitting in these cell types is slowly being elucidated. Cody and Mountain [5] have demonstrated that peak-splitting in low-frequency responses of IHCs arises from the mechanical input to the IHC, i.e. the vibrations of the basilar membrane (BM) relative to the tectorial membrane. Furthermore, the IHCs provide the inputs to AN fibres and so it is clear that AN fibre low-frequency responses will show similar peak-splitting to that seen in IHC responses. It is theoretically possible, however, for AN fibres to show peak-splitting in their low-frequency responses even when there is no peak-splitting present in the attached IHC low-frequency responses. If this were to occur, then it is likely to arise as a result of non-linearities associated with the way in which a AN fibre processes its IHC input. Cai and Geisler [1] demonstrated that peak-splitting in AN fibre responses was unpredictable, thus giving strong indication of non-linear effects. Cochlear nucleus (CN) neurons, which receive inputs from AN fibres, are also thought to demonstrate peak-splitting in their response to low-frequency tones. The goal of the present study is to understand how peak-splitting in the low-frequency responses of CN neurons depends on neuronal parameters, such as the spiking-rate of individual input AN fibres and the amplitude of the input excitatory postsynaptic potentials (EPSPs). To achieve this goal a leaky integrate-and-fire (LIF) single neuron model of a CN neuron receiving stochastic periodic AN fibre inputs was implemented. In this model input EPSPs to the neuron are summed and an action potential (AP or spike) is generated when the membrane potential reaches threshold.

II. METHODS

II.1. Neural Model

The analysis presented here considers a single neuron with N independent inputs (afferent fibres) assumed to have the same synaptic response amplitude, a, and time course, $s(t)$. The time course of an input at the site of spike generation is described by the synaptic response function $u(t)$ for the LIF neuron model. The membrane potential is assumed to be reset to its initial value at time $t = 0$, $V(0) = v_0$, after an AP has been generated. An AP is produced only when the membrane potential exceeds the threshold, $V_{\rm th}$, which has a potential difference with the reset potential of $\theta = V_{\rm th} - v_0$. After an AP has been generated there is an absolute refractory period, τ_r, during which no APs can be generated. The mem-

brane potential is the sum of the input EPSPs

$$V(t) = v_0 \; + \; N\, a\; s(t), \;\; s(t) = \sum_{m=1}^{\infty} u(t - t_m), \qquad (1)$$

where the index m denotes the m^{th} input AP from the particular fibre, whose time of arrival is t_m ($0 < t_1 < t_2 < ... < t_m < ...$). The rate of the input AP arrival times is discussed in the following section. The synaptic response function, $u(t)$, is

$$u(t) \quad = \quad \begin{cases} e^{-t/\tau} & \text{for } t \geq 0 \\ 0 & \text{for } t < 0, \end{cases} \qquad (2)$$

where τ is the decay time constant of the membrane potential. Consequently the membrane potential has a discontinuous jump of size a upon the arrival of an EPSP and then decays exponentially between inputs. The decay of the EPSP across the membrane means that the contribution from EPSPs that arrive earlier have partially decayed by the time that later EPSPs arrive. In this study the voltage scale is set so that $v_0 = 0$.

II.2. Synaptic Input

In this study it is assumed that the input spiking-rate on each of the input fibres is identical. The time-dependent rate of arrival of input spikes at a synapse is periodic with period T and initial phase t_ϕ,

$$\lambda(t) = p\left(\sum_{k=-\infty}^{\infty} \frac{1}{\sqrt{2\pi\sigma^2}} \exp\left(-\frac{(t - kT + t_\phi)^2}{2\sigma^2}\right)\right), \quad (3)$$

where, for a single fibre, p is the time-averaged input spiking-rate per period and σ is the standard deviation (S.D.) of the Gaussians. The synchronization index (SI - a measure of the degree of locking to a phase of the period of the input [10]) of the above spiking-rate function, denoted S, can be calculated as follows [11],

$$S = \exp\left(-\frac{2\pi^2\sigma^2}{T^2}\right). \qquad (4)$$

This expression for S can be calculated by dividing the first complex Fourier coefficient of $\lambda(t)$ by the zeroeth complex Fourier coefficient of $\lambda(t)$. The period, T, and the S.D. of the Gaussians, σ, can be varied independently to provide the desired S value. The use of the term "period" (or "frequency" $\text{f} = \frac{1}{T}$) here and throughout the analysis refers to this periodic modulation of the spiking-rate of the inputs. Furthermore, for the sake of using conventional terms, the average spiking-rate per input can be defined as $\lambda_{\text{in}} = \frac{p}{T}$. This input spiking-rate function, Equation (3), represents an inhomogeneous Poisson process [12].

II.3. Output of the Model

Now that the neural model and its synaptic inputs have been defined, the output of the model can be evaluated by using the following methods developed by Burkitt and Clark [13], [14], [15]. Based on a description of the membrane potential and the synaptic inputs, one can now temporally integrate the synaptic inputs and the probability density of the membrane potential can be obtained in the Gaussian approximation. Using a generalization of the renewal equation, the probability density of the membrane potential and the probability density of the membrane potential conditional on the initial phase of the inputs can be used to evaluate the conditional first-passage time density (equivalent to the inter-spike interval distribution conditional on the initial phase of the inputs). The output of the model, the phase distribution (synonymous with the phase histogram), can then be evaluated. The phase distribution is the stationary solution to a phase transition density defined by the periodic wrapping of the conditional first-passage time densities [15], [16]. As a result of obtaining the phase distribution, the SI of the model's output can be evaluated numerically [10].

III. RESULTS

Peak-splitting was observable in the output phase distributions of the LIF neuron model. It arose as a result of an increase in the average spiking-rate per period of the input, p. Fig. 1 demonstrates the appearance of peak-splitting in the output phase distribution as a result of this increase of average input spiking-rate. The ordinate represents the spike phase density, $\chi(t_\phi)$ (where t_ϕ is the phase at which an AP is produced), and the abcissa represents the time for one stimulus period. All model parameter values are given in the figure caption. In Fig. 1(a) and (b) the average spiking-rate per input is $\lambda_{\text{in}} = 300$ and 800 spikes/s respectively (i.e. $p = 1$ and 4 spikes/period), the output SI is $S_{\text{out}} = 0.95$ and 0.57 respectively and the average output spiking-rate is $\lambda_{\text{out}} = 50.81$ and 282.04 spikes/s respectively. As the input spiking-rate increases, the phase distribution spreads to the right and eventually the original peak splits into two, with the two resulting peaks being 1.61 ms apart.

Peak-splitting was also found to occur by increasing EPSP amplitude, a, while keeping the average spiking-rate per input fixed. Fig. 2 demonstrates the appearance of peak-splitting in the output phase distribution as a result of an increase in a. The ordinate represents the spike phase density, $\chi(t_\phi)$, and the abcissa represents the time for one stimulus period. All model parameter values are given in the figure caption. For Fig. 2(a) and (b) the EPSP amplitude is $a = 0.05$ and 0.25 respectively, the output SI is $S_{\text{out}} = 0.95$ and 0.55 respectively and the average output spiking-rate is $\lambda_{\text{out}} = 50.81$ and 531.39 spikes/s respectively. As the EPSP amplitude increases, the phase distribution spreads to the right and eventually the original peak splits into two, with the two resulting peaks being 1.24 ms apart.

IV. DISCUSSION

As was demonstrated in Fig. 1 and Fig. 2 peak-splitting in the output of the model was shown to

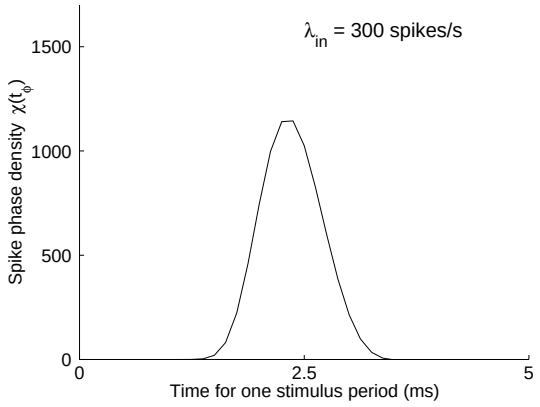

(a)

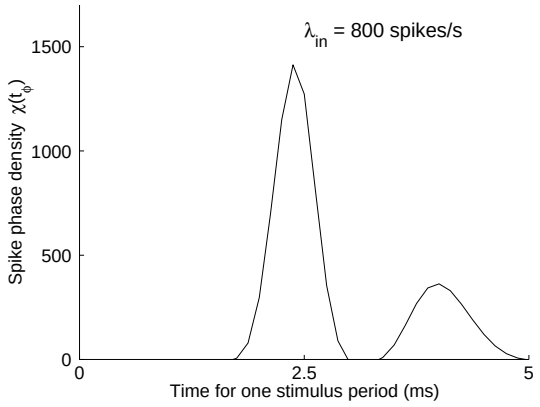

(b)

Fig. 1. Plots of phase distributions demonstrating the appearance of peak-splitting as a result of an increase in average spiking-rate per input. The ordinate represents the spike phase density, $\chi(t_\phi)$, and the abcissa represents the time for one stimulus period, measured in milliseconds (ms). The neural parameter values are, $N = 20$ inputs, $a = 0.05$, $\theta = 1$, $\tau_r = 1$ ms and $\tau = 2$ ms. The input parameter values are, $T = 5$ ms and $S_{\text{in}} = 0.5$. For (a) and (b) the average spiking-rate per input is $\lambda_{\text{in}} = 300$ and 800 spikes/s respectively (i.e. $p = 1.5$ and 4 spikes/period), the output SI is $S_{\text{out}} = 0.92$ and 0.57 respectively and the average output spiking-rate is $\lambda_{\text{out}} = 50.81$ and 282.04 spikes/s respectively.

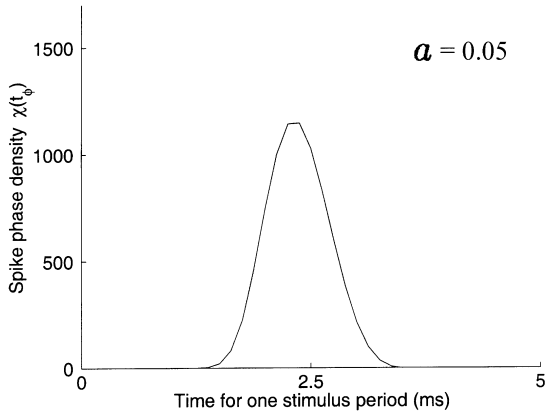

(a)

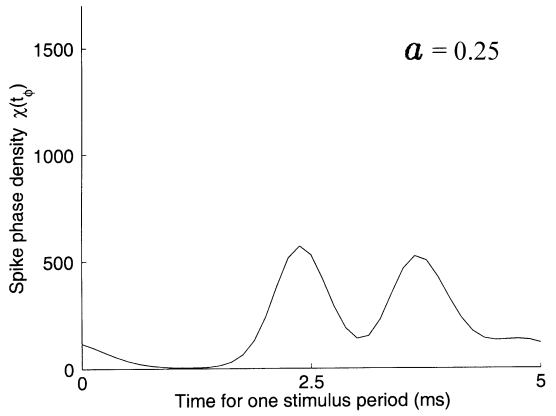

(b)

Fig. 2. Plots of phase distributions demonstrating the appearance of peak-splitting in the output phase distribution as a result of an increase in the EPSP amplitude, a. The ordinate represents the spike phase density, $\chi(t_\phi)$, and the abcissa represents the time for one stimulus period, measured in milliseconds (ms). The neural parameter values are, $N = 20$ inputs, $\theta = 1$, $\tau_r = 1$ ms and $\tau = 2$ ms. The input parameter values are, $T = 5$ ms, $\lambda_{\text{in}} = 300$ spikes/s ($p = 1.5$ spikes/period) and $S_{\text{in}} = 0.5$. For (a) and (b) the EPSP amplitude is $a = 0.05$ and 0.25 respectively, the output SI is $S_{\text{out}} = 0.95$ and 0.55 respectively and the average output spiking-rate is $\lambda_{\text{out}} = 50.81$ and 531.39 spikes/s respectively.

occur as a result of an increase in the average spiking-rate per input, λ_{in}, and an increase in the EPSP amplitude of the inputs, a, respectively. An increase in the average spiking-rate per input, λ_{in}, effectively corresponds to an increase in stimulus intensity. As is shown in Fig. 1 for a stimulus frequency of 200 Hz, a seemingly unrealistic value for the average spiking-rate per input is required in order for peak-splitting to occur. In Fig. 1 an average spiking-rate per input of $\lambda_{\text{in}} = 800$ spikes/s is required for peak-splitting to occur. Clearly, as a result of the typical refractory period of a neuron (of the order of 1 ms (see [17] for a review), such a value for the average input spiking-rate does not appear realistic. However, given the design of the LIF neuron model presented here, the total number of input spikes per second, i.e. $N \times \lambda_{\text{in}}$, ultimately determines the output response. Thus it is possible that the peak-split response seen in Fig. 1 may arise in a situation where there are more inputs than in Fig. 1 and the spiking-rate of individual inputs increases in a realistic manner such that the total number of input spikes per second is the same as in Fig. 1. In Fig. 2, where the occurrence of peak-splitting is demonstrated for an increase in EPSP amplitude, seemingly realistic values of the EPSP amplitude relative to the size of the cell's threshold are required for peak-splitting to occur. In Fig. 2 the value of a for which peak splitting occurs is one quarter of the threshold. Considering that the neural model represents a CN neuron, such a value for the EPSP amplitude appears to be realistic [18], [19].

The height, shape and number of the peaks in the phase distribution depends on several of the parameters of the model. The height and shape of each peak depends largely on the parameters that determine the SI of the output (results not presented here). The number of peaks depends on the average input

spiking-rate and input EPSP amplitude, as is discussed in this section, where an increase in the values of these parameters acts to increase the probability that the model neuron will spike more than once per period. The relative position of the peaks in the phase distribution may correspond to higher order harmonics of the input frequency.

V. CONCLUSION

As was discussed in the introduction, peak-splitting research has concentrated on IHCs [4], [5] and AN fibres [1], [2], [3], [4], [6], [7], [8], [9]. These studies have primarily demonstrated that the peak-splitting in response to low-frequency tones that occurs in BM vibrations is preserved in the response of IHCs and AN fibres. In the present study, it seems clear that peak-splitting can be generated in a CN neuron's response to low-frequency tones not only in this situation, but also in the situation where there is no peak-splitting in BM vibrations or the input AN fibre responses, but rather by an increase in the EPSP amplitude, or both the EPSP amplitude and the average spiking-rate, of the input AN fibres. This idea warrants further investigation using a compartmental model of CN neurons of the type used by Rothman *et al.* [18], [19]. In fact Rothman *et al.* noted that peak-splitting occurred in their model when each input was suprathreshold. This is consistent with the work presented here where large amplitude, but not necessarily suprathreshold, EPSPs are required to induce peak-splitting.

Much is known about the way that components of the auditory pathway code sounds in the times of their responses. However, the role that peak-splitting plays in temporal coding in the auditory pathway is not quite clear. It is hoped that future studies will help to elucidate this role.

VI. ACKNOWLEDGEMENTS

The authors would like to thank A. Paolini and B. Uragun for their useful comments on the manuscript.

References

[1] Cai, Y., & Geisler, C. D. 1996. Temporal patterns of the responses of auditory-nerve fibers to low-frequency tones. *Hearing Res.*, **96**, 83–93.

[2] Kiang, N. Y. S., & Moxon, E. C. 1972. Physiological considerations in artificial stimulation of the inner ear. *Ann. Otol.*, **81**, 714–730.

[3] Johnson, D. H. 1980. The Relationship Between Spike Rate and Synchrony in Responses of Auditory-Nerve Fibers to Single Tones. *J. Acoust. Soc. Am.*, **68**, 1115–1122.

[4] Palmer, A. R., & Russell, I. J. 1986. Phase-locking in the cochlear-nerve of the guinea-pig and its relation to the receptor potential of inner hair cells. *Hearing Res.*, **24**, 1-15.

[5] Cody, A. R., & Mountain, D. C. 1989. Low-frequency responses of inner hair cells: evidence for a mechanical origin of peak splitting. *Hearing Res.*, **41:2-3**, 89–99.

[6] Ruggero, M. A., Robles, L., & Rich, N. C. 1986. Cochlear microphonics and the initiation of spikes in the auditory nerve: correlation of single-unit data with neural and receptor potentials recorded from the round window. *J. Acoust. Soc. Am.*, **79:5**, 1491–1498.

[7] Kiang, N. Y. S. 1990. Curious oddments of auditory-nerve studies. *Hearing Res.*, **49:1-3**, 1–16.

[8] Joris, P. X., & Yin, T. C. T. 1992. Responses to amplitude-modulated tones in the auditory nerve of the cat. *J. Acoust. Soc. Am.*, **91:1**, 215–232.

[9] Ruggero, M. A., Rich, N. C., Shivapuja, B. G., & Temchin, A. N. 1995. Auditory-nerve responses to low-frequency tones: intensity dependence. *Aud. Neurosci.*, **2:2**, 159–186.

[10] Goldberg, J. M., & Brown, P. B. 1969. Response of Binaural Neurons of Dog Superior Olivary Complex to Dichotic Tonal Stimuli: Some Physiological Mechanisms of Sound Localization. *J. Neurophysiol.*, **32**, 613–636.

[11] Kempter, R., Gerstner, W., van Hemmen, J. L., & Wagner, H. 1998. Extracting Oscillations: Neuronal Coincidence Detection with Noisy Periodic Spike Input. *Neural Comput.*, **10**, 1987–2017.

[12] Papoulis, A. 1991. *Probability, Random Variables, and Stochastic Processes*. Singapore: McGraw-Hill International Editions. 3rd Edition.

[13] Burkitt, A. N., & Clark, G. M. 1999a. Analysis of Integrate-and-Fire Neurons: Synchronization of Synaptic Input and Spike Output in Neural Systems. *Neural Comput.*, **11**, 871–901.

[14] Burkitt, A. N., & Clark, G. M. 2000a. Calculation of Interspike Intervals for Integrate and Fire Neurons with Poisson Distribution of Synaptic Inputs. *Neural Comput.*, **12**, 1789–1820.

[15] Burkitt, A. N., & Clark, G. M. 2000b. Synchronization of the Neural Response to Noisy Periodic Synaptic Input. *Manuscript submitted.*

[16] Plesser, H. E., & Geisel, T. 1999. Bandpass Properties of Integrate-Fire Neurons. *Neurocomputing*, **26/27**, 229–235.

[17] Koester, J. Voltage-Gated Ion Channels and the Generation of the Action Potential. In Kandel, E. R., Schwartz, J. H., & Jessel, T. M., editors, *Principles of Neural Science*, chapter 8, pages 104-118. Appleton & Lange, Connecticut, third edition, 1991.

[18] Rothman, J. S., Young, E. D., & Manis, P. B. 1993. Convergence of Auditory Nerve Fibers Onto Bushy Cells in the Ventral Cochlear Nucleus: Implications of a Computational Model. *J. Neurophysiol.*, **70**, 2562–2583.

[19] Rothman, J. S., & Young, E. D. 1996. Enhancement of Neural Synchronization in Computational Models of Ventral Cochlear Nucleus Bushy Cells. *Aud. Neurosci.*, **2**, 47–62.

Author/s:
KUHLMANN, L;BURKITT, AN;CLARK, GM

Title:
Peak-Splitting in the Response of the Leaky Integrate-and-Fire Neuron Model to Low-Frequency Periodic Inputs

Date:
2001

Citation:
KUHLMANN, L., BURKITT, A. N. & CLARK, G. M. (2001). Peak-Splitting in the Response of the Leaky Integrate-and-Fire Neuron Model to Low-Frequency Periodic Inputs. Proceedings of the IEEE Engineering in Medicine and Biology Society Conference, pp.1-4. Monash University Press.

Persistent Link:
http://hdl.handle.net/11343/27084